JACS
JOURNAL OF THE AMERICAN CHEMICAL SOCIETY
Article
pubs.acs.org/JACS

# Molecular Orientation of Enzymes Attached to Surfaces through Defined Chemical Linkages at the Solid–Liquid Interface

Yuwei Liu, Tadeusz L. Ogorzalek, Pei Yang, McKenna M. Schroeder, E. Neil G. Marsh,* and Zhan Chen*

Department of Chemistry, University of Michigan, Ann Arbor, Michigan 48109, United States

Supporting Information

**ABSTRACT:** The immobilization of enzymes on solid supports is widely used in many applications, including biosensors, antifouling coatings, food packaging materials, and biofuel cells. Enzymes tend to lose their activity when in contact with a support surface, a phenomenon that has been attributed to unfavorable orientation and (partial) unfolding. In this work, specific immobilization of 6-phospho-$\beta$-galactosidase ($\beta$-Gal) on a self-assembled monolayer (SAM) containing maleimide end groups and oligo(ethylene glycol) spacer segments was achieved through a unique cysteinyl residue. A systematic means to characterize the interfacial orientation of immobilized enzymes has been developed using a combination of sum frequency generation vibrational spectroscopy and attenuated total reflectance FTIR-spectroscopy. The possible orientations of the immobilized $\beta$-Gal were determined and found to be well-correlated with the tested activity of $\beta$-Gal. This study will impact the development of an increasingly wide range of devices that use surface-immobilized enzymes as integral components with improved functions, better sensitivity, enhanced stability, and longer shelf life.

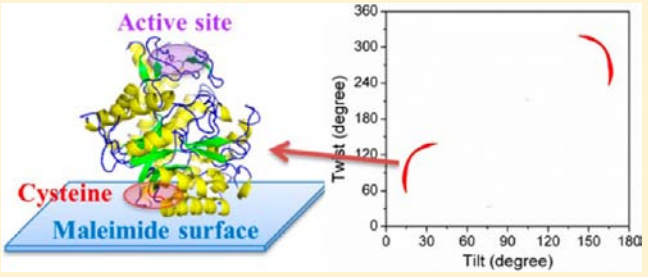


## 1. INTRODUCTION

The immobilization of enzymes on solid supports[1−4] has found many applications ranging from biosensors used in energy and medical fields to other biocatalyst carriers such as antifouling coatings, food packaging materials, and biofuel cells.[5−16] The advantages of using immobilized enzymes as opposed to enzymes in free solution include improved stability, reusability, and localization. These features allow better control of manufacturing processes and reduce production costs by efficiently recycling the enzymes.[4,17] Additionally, the architecture, and chemical and mechanical properties of solid supports can be manipulated to improve the loading capacity and modulate the selectivity and activity of the attached enzymes.[10,18−20] Advances in molecular biology such as the availability of gene synthesis have made it possible to easily tailor enzymes to facilitate various immobilization strategies.

A number of techniques have been used for enzyme immobilization, including entrapment, encapsulation, surface immobilization through non-covalent bonds such as physical adsorption (hydrophobic–hydrophobic interaction) or ionic binding, and last, covalent attachment to the surface.[1,13,21] Physical adsorption is commonly used because of its simplicity. However, the non-covalent nature of physical adsorption often results in leaching of enzyme from the surface over time. Leaching is prevented by covalent binding of the enzyme to appropriately functionalized surfaces. A frequently used approach involves cross-linking the enzyme to the surface through lysine residues on the protein using reagents such as glutaraldehyde or carbodiimides.[4,8] However, because proteins typically have multiple lysine residues, this leads to random surface orientation, multiple cross-links, and often unfolding, all of which reduce the enzyme activity. A more specific approach involves tethering the enzyme through cysteine residues, which are infrequently found on the exterior of proteins and can be chemically linked to maleimide-functionalized surfaces. Unique cysteine residues can easily be introduced into the enzyme at a well-defined position on the protein's surface by mutagenesis. This in principle allows the orientation of the enzyme with respect to the surface to be controlled.

Enzymes tend to lose their activity when in contact with a support surface,[22−24] a phenomenon that has been attributed to unfavorable orientation and (partial) unfolding. However, detailed information about the structure and orientation of surface-immobilized enzymes remains lacking because of the technical difficulties associated with characterizing a single layer of enzyme molecules on a surface. To address this problem, we have used surface-sensitive vibrational spectroscopic techniques such as sum frequency generation spectroscopy (SFG), which involves a second-order nonlinear optical process and is intrinsically surface-sensitive.[25−33] It has been shown to be an extremely powerful tool for studying the secondary structures and orientations of interfacial peptides and proteins.[34−50] Attenuated total reflectance-Fourier transform infrared spectroscopy (ATR-FTIR) provides another technique to study peptide or protein interfacial structure and orientation with a penetration depth of a few micrometers.[51−54] A combination of SFG and ATR-FTIR has been used to determine complicated

Received: April 12, 2013
Published: July 24, 2013

   dx.doi.org/10.1021/ja403672s | J. Am. Chem. Soc. 2013, 135, 12660−12669

orientations of peptides and the orientation of complex proteins.[55−57]

In the present study, we used 6-phospho-β-galactosidase (β-Gal) from *Lactococcus lactis* as a model enzyme for which detailed structural and kinetic information is available.[58] We engineered this enzyme to contain a unique surface cysteine residue on the side of the enzyme opposite to the active site. This allowed the protein to be attached through a unique, chemically defined linkage to a chemically well-defined surface, in this case a maleimide-terminated self-assembled monolayer (SAM) assembled on a silica surface.[43,59−61] We investigated the orientation of the enzyme with respect to the surface normal using SFG and ATR-FTIR and examined how attaching the enzyme to the surface changes its activity.

## 2. MATERIALS AND METHODS

All of the chemicals and reagents were purchased from Sigma-Aldrich (St. Louis, MO, USA) and used without further purification unless otherwise stated.

**2.1. β-Gal Constructs and Expression of Modified β-Gal.** A synthetic gene codon-optimized for expression in *Escherichia coli* and encoding β-Gal from *L. lactis* (PDB entry 2PBG)[58] was obtained commercially (Genscript, New Jersey) and subcloned into the expression vector pET28b so as to contain an N-terminal His tag. The sequence was modified to replace all of the native cysteine residues with alanine. In addition, Val-152 was mutated to cysteine. A second construct containing no cysteine was made by using site-directed mutagenesis to mutate Cys-152 back into a valine.

Expression vectors containing the β-Gal gene were transformed into *E. coli* BL21(DE3). Cells were grown in YT medium containing 50 μg/mL kanamycin to an optical density of 0.6 at 600 nm. Protein expression was induced by addition of 100 μM isopropyl β-D-1-thiogalactopyranoside (IPTG). The cell culture was harvested 4 h post induction by centrifugation at 5000*g* at 4 °C for 20 min.

**2.2. Purification of Recombinant β-Gal.** Cells (18 g damp weight) were resuspended in 90 mL of 100 mM Tris buffer (pH 8.0) containing 300 mM NaCl, 10 mM imidazole, 10% glycerol, 1 mM tris(2-carboxyethyl)phosphine (TCEP), and a complete EDTA-free protease inhibitor cocktail tablet (Roche). Resuspended cells were sonicated using a 2 s on/8 s off pulse sequence for a total pulse time of 5 min. The lysate was centrifuged at 15000*g* at 4 °C for 20 min, and the supernatant from the lysate was incubated with 4 mL of Ni-NTA resin at 4 °C for 1 h. The Ni-NTA resin was then decanted into a chromatography column and washed with 50 mL of 20 mM imidazole dissolved in a 100 mM potassium phosphate buffer (pH 8) containing 300 mM NaCl, 10% glycerol, and 1 mM TCEP. β-Gal was eluted from the column using 10 mL of 200 mM imidazole dissolved in 100 mM potassium phosphate buffer (pH 8) containing 300 mM NaCl, 10% glycerol, and 1 mM TCEP. Fractions with pure enzyme were collected and dialyzed into 100 mM potassium phosphate buffer (pH 7.6) containing 10% glycerol and 1 mM TCEP. The enzyme was then concentrated using Amicon Ultra-15 centrifugal filters to a concentration of 50−100 μM and stored frozen at −20 °C.

**2.3. Enzyme Assay.** The β-Gal activity was tested using either the fluorogenic substrate fluorescein β-digalactopyranoside (FDG) or the chromogenic substrate 2-nitrophenyl-β-galactopyranoside. The assay buffer typically contained 100 mM potassium phosphate (pH 7.6), 1 mM $MgCl_2$, 1 mM 2-mercaptoethanol, and 1% dimethyl sulfoxide (DMSO). For 2-nitrophenyl-β-galactopyranoside, the substrate concentrations varied between 0 and 1 mM, and the release of 2-nitrophenol was followed by the change in absorption at 412 nm. Assays using FDG were conducted at a concentration of 200 μM; the excitation wavelength was 490 nm, and the emission spectra were scanned from 500 to 550 nm to detect release of fluorescein. When FDG was used as the substrate, the concentration of β-Gal was typically 10 nM; for assays using 2-nitrophenyl-β-galactopyranoside as the substrate, the enzyme concentration was 1 μM.

To determine the activity of β-Gal immobilized on glass beads, the assay was modified as follows. Glass beads loaded with 10 pmol of β-Gal were added to a cuvette containing 990 μL of 100 mM potassium phosphate buffer (pH 7.6) containing 1 mM $MgCl_2$. The reaction was started by adding 10 μL of FDG in DMSO to final concentrations of 200 μM FDG and 1% DMSO. The cuvette was shaken gently at room temperature to keep the beads suspended, and fluorescence measurements were taken discontinuously every 2 min for 30 min, allowing a short time for the beads to settle before the measurement was taken.

**2.4. Substrate Functionalization/SAM Preparation.** Right-angle $CaF_2$ prisms purchased from Altos Photonics (Bozeman, MT, USA) were soaked in toluene for 24 h and then sonicated in 1% Contrex AP solution (Decon Laboratories, King of Prussia, PA, USA) for 10 min. The prisms were thoroughly rinsed with Millipore water (18.2 MΩ cm), dried under $N_2$, and placed into an oxygen benchtop plasma cleaner (PE-25-JW, Plasma Etch, Carson City, NV, USA) for 4 min immediately before being coated with $SiO_2$. A 100 nm layer of $SiO_2$ was deposited onto the $CaF_2$ prisms by an electron-beam deposition process using an SJ-26 evaporator system at a pressure below $10^{-5}$ Torr. The deposition rate was 5 Å/s.

The $SiO_2$-coated $CaF_2$ prisms were treated with the $O_2$ plasma cleaner for 4 min. These clean prisms were placed in freshly made 1 mM maleimide-EG4-silane (Mal-EG4) (Creative PEGWorks, Winston Salem, NC, USA) or octadecyltrichlorosilane (OTS) in anhydrous toluene for 24 h at room temperature. The molecular structures of Mal-EG4 and OTS are shown in Figure 1A. The functionalized prisms were rinsed with copious amounts of toluene followed by methanol and dried under vacuum for 1 h. The Mal-EG4 SAM was characterized using X-ray photoelectron spectroscopy (XPS); more details can be found in the Supporting Information.

**2.5. SFG Experiment and Data Analysis.** The SFG setup used in this study was purchased from EKSPLA. Details of the setup can be obtained from the manufacturer, and some details have been described in previous publications[34,36−42,57,62−70] and will not be reiterated here. SFG is a second-order nonlinear optical process that probes systems with no inversion symmetry under the electric dipole approximation. Since most bulk materials have inversion symmetry, SFG is an intrinsically surface-sensitive technique that provides submonolayer surface sensitivity. In this study, a near-total-reflection geometry (Figure 1B) was used, in which the two input laser beams were directed through one face of a right-angle $CaF_2$ prism and overlapped on the other face, which was coated with a Mal-EG4 SAM grown on a deposited $SiO_2$ thin layer. This surface was in contact with a reservoir containing 2 mL of 5 mM phosphate buffer (pH 7.2) and 0.1 mM TCEP. An enzyme stock solution to which 1 mM TCEP had been added was incubated with gentle shaking at room temperature for 2 h to reduce potential disulfide bonds. The appropriate volume of this enzyme stock solution was injected to the reservoir to give a concentration of 4 μM. The reservoir was stirred at a rate of 125 rpm using a magnetic microstir bar to ensure a homogeneous concentration distribution of enzyme molecules in the subphase below the prism. After the system was equilibrated, SFG spectra with polarization combinations of ssp (s-polarized sum frequency output, s-polarized visible input, and p-polarized IR input) and ppp were collected and used for orientation analysis. All of the SFG spectra were normalized according to the intensities of the input IR and visible beams.

The primary experimentally measured quantity used for orientation analysis in the present SFG studies was the ratio of the effective second-order nonlinear optical susceptibility tensor components detected in the ppp and ssp polarizations ($\chi^{(2)}_{zzz}/\chi^{(2)}_{xxz}$). Methods of determining the molecular orientations of single peptides and larger proteins have been reported previously.[38,40,41,66,68−70] We previously developed a computer program that performs these calculations in a semiautomated fashion for proteins that contain many α-helices, and this program makes it possible to characterize the orientation of complex molecules in terms of the tilt angle ($\theta$) and twist angle ($\psi$).[41,56] More details regarding the SFG data analysis can be found in the Supporting Information.

**2.6. ATR-FTIR Experiment and Data Analysis.** ATR-FTIR experiments were carried out with a Nicolet Magna 550 FTIR

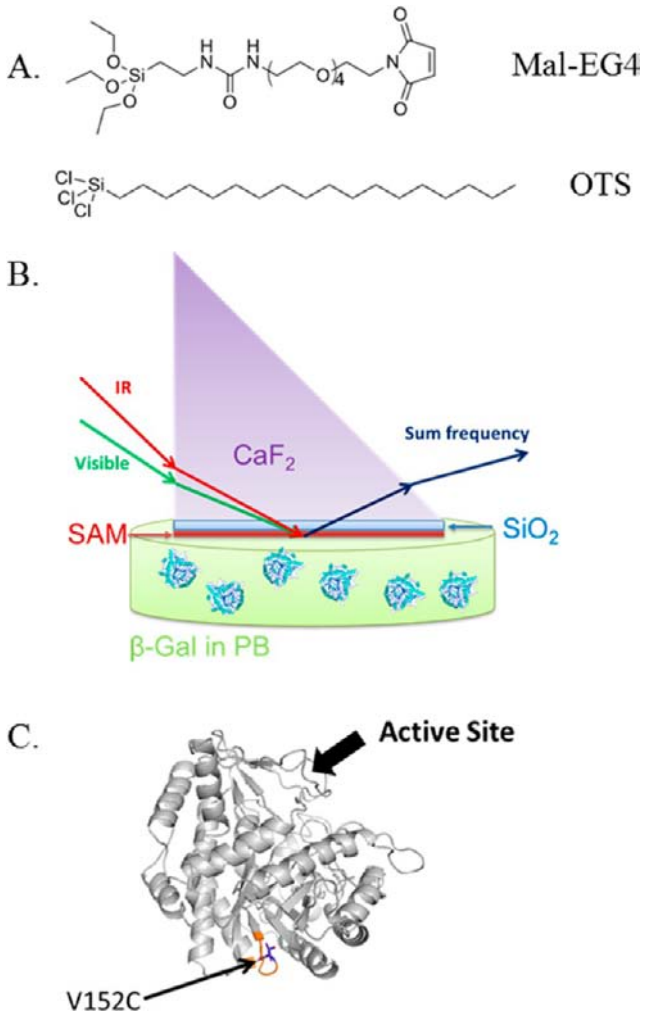


**Figure 1.** (A) Molecular formulas of Mal-EG4 and OTS. (B) SFG experimental geometry used in this study. This is a near-total-reflection geometry. Tunable IR and fixed visible (532 nm) laser beams travel through one face of a right-angle $CaF_2$ prism and overlap on the other face, which is coated with a Mal-EG4 SAM grown on a deposited $SiO_2$ thin layer. This surface is in contact with a reservoir of buffer solution containing enzyme molecules. (C) Crystal structure of $\beta$-Gal-V152C, in which the valine at position 152 is replaced by a cysteine group. This cysteine can bind to a maleimide group on the Mal-EG4 SAM to immobilize $\beta$-Gal to the surface. The binding site is on the side opposite to the enzyme active site.

spectrometer using a detachable ZnSe total-internal-reflection crystal (Specac Ltd., Slough, England). The ZnSe crystal surface was cleaned with methanol, 1% Contrex AP solution, and Millipore water and then treated in the $O_2$ plasma chamber for 2 min immediately before electron-beam deposition of a 50 nm $SiO_2$ layer as described above. The $SiO_2$-coated ZnSe crystal was treated in the $O_2$ plasma chamber for 2 min, and the same procedure was followed to functionalize the surface of the ZnSe crystal with Mal-EG4. After the SAM was formed on the crystal, pH 7.2 phosphate buffer and TCEP solution in $D_2O$ were added to the 1.6 mL trough above the crystal to reach final concentrations of 5 and 0.1 mM, respectively. $D_2O$ was used to avoid possible signal confusion between the O−H bending mode and the peptide amide-I mode and to ensure a better signal-to-noise ratio in the peptide amide-I band region. After the background spectra were recorded, the appropriate volume of an enzyme stock solution (incubated with 1 mM TCEP to reduce potential disulfide bonds as described above) was injected into the subphase to achieve the desired enzyme concentration of 4 $\mu$M. The s- and p-polarized ATR-FTIR spectra of the enzyme interacting with SAM were recorded for orientation analysis after the system reached equilibrium.

We also developed a computer program similar to the SFG data analysis program to analyze ATR-FTIR data.[56] This program was used to analyze the ATR-FTIR spectra to relate the protein orientation to the dichroic ratio $R^{ATR}$, which is related to the fitted peak intensities (or integrated absorbances) of the peaks with parallel and perpendicular polarizations, respectively.

To enable direct comparisons between the ATR-FTIR and SFG orientation analysis methodologies for $\alpha$-helices, we previously derived the helical orientation relations for ATR-FTIR using a consistent set of rotation conventions.[56] Because of the large number of terms in the resulting equations, the algebraic details are not presented here, but these equations were directly integrated into the computer software for SFG and ATR-FTIR data analysis.[56]

## 3. RESULTS AND DISCUSSION

6-Phospho-$\beta$-galactosidase ($\beta$-Gal) from *L. lactis* was chosen as a model enzyme for this research because it is predicted to generate a large SFG signal due to its $\alpha$-helical structure (on the basis of calculations using the computer software discussed above). Previous reports had demonstrated that the enzyme maintains activity when immobilized on various solid supports via physical adsorption, covalent binding, chemical aggregation, encapsulation, and entrapment to increase its stability and reusability.[71−77] The activity of $\beta$-Gal can be assayed using commercially available chromogenic or fluorogenic substrates, providing simple and sensitive ways to investigate the effects of immobilization on the activity. The enzyme adopts a $\beta_8/\alpha_8$-barrel fold[58] (PDB entry 2PBG) with all of the $\alpha$-helixes pointing in approximately the same direction (Figure 1C). This is important because it allows the orientation of the immobilized enzyme with respect to the surface to be experimentally determined by SFG.

**3.1. Engineering of $\beta$-Gal.** Native $\beta$-Gal contains three cysteine residues, none of which are required for activity.[58] In addition, the enzyme contains no disulfide bonds that could be required for structural stability. Therefore, a synthetic gene was constructed in which all three native cysteine residues were mutated to alanine. Next, to facilitate tethering of the enzyme to a maleimide-terminated SAM, Val-152 was mutated to cysteine. Position 152 is on a surface loop (Figure 1C) and was chosen to minimize any disruption of the secondary structure that covalent attachment of the enzyme to the surface may cause. Furthermore, it should orient the active site to face toward the bulk solvent, providing the substrate easy access to the active site. A second construct containing no surface cysteine residues was also made. In this case, site directed mutagenesis was used on the original synthetic gene to revert Cys-152 back to a valine. Both the "no cysteine" and $\beta$-Gal-V152C enzymes were overexpressed and purified from *E. coli* by standard methods.

The kinetic parameters $k_{cat}$ and $K_m$ for both $\beta$-Gal enzymes, free in solution, were measured for the hydrolysis of the chromogenic substrate 2-nitrophenyl-$\beta$-galactopyranoside. For the $\beta$-Gal-V152C enzyme variant, $k_{cat} = 0.18 \pm 0.01$ s$^{-1}$ and $K_m = 0.2 \pm 0.02$ mM; for the "no cysteine" $\beta$-Gal enzyme variant, $k_{cat} = 0.35 \pm 0.03$ s$^{-1}$ and $K_m = 0.1 \pm 0.01$ mM. These values are similar to those reported for the wild-type enzyme,[58] indicating that the engineered changes did not substantially affect the activity of the enzyme. The presence of a single reactive cysteine residue in $\beta$-Gal-V152C was confirmed using 5,5′-dithiobis(2-nitrobenzoic acid) (Ellman's reagent). The


dx.doi.org/10.1021/ja403672s | J. Am. Chem. Soc. 2013, 135, 12660−12669

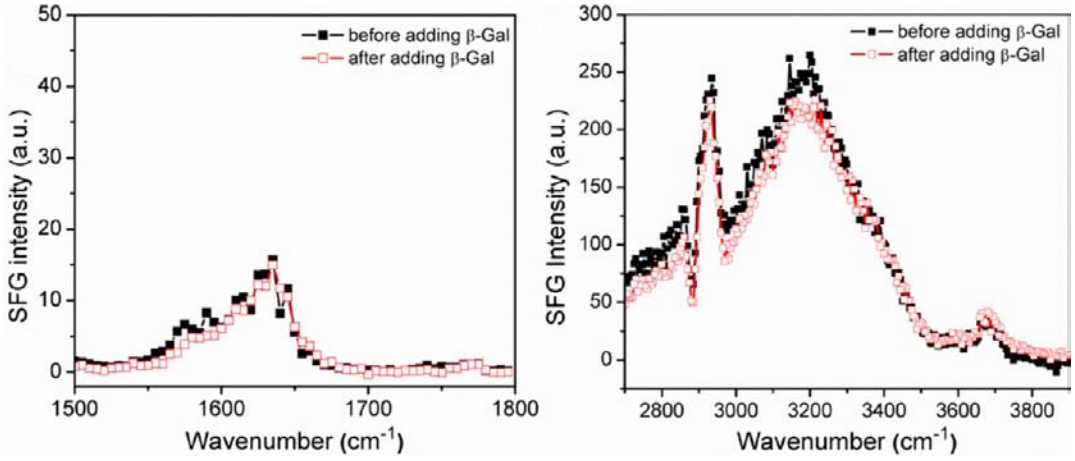


**Figure 2.** (left) Amide-I and (right) C−H/O−H stretching frequency regions of SFG ssp spectra collected from the Mal-EG4−buffer solution interface before (black ■) and after (red □) introduction of the "no cysteine" $\beta$-Gal variant to the buffer solution. The spectra before and after the addition of "no cysteine" $\beta$-Gal are similar, indicating no physical adsorption of $\beta$-Gal on the Mal-EG4 surface.

method for surface cysteine determination can be found in the Supporting Information.

**3.2. SFG and ATR-FTIR Experiments and Data Analysis for $\beta$-Gal on the Mal-EG4 SAM.** *3.2.1. Evidence of Elimination of Nonspecific Binding with EG4 Segments.* To prevent or minimize the physical adsorption of $\beta$-Gal molecules on the surface, oligo(ethylene glycol) (OEG) "spacer" groups were incorporated into the molecules used to form the SAM.[60,78,79] Previous studies have shown that both tightly bound water associated with the OEG chains and their high flexibility play important roles in preventing nonspecific protein adhesion.[78,80−82] SFG ssp spectra were collected from the interface of the Mal-EG4 SAM and the buffer solution before and after the addition of "no cysteine" $\beta$-Gal. The similarity of spectra in the amide-I region (Figure 2) showed that either no enzyme was adsorbed onto the SAM surface or the adsorbed enzymes were randomly oriented. However, the similarity of the spectra in the C−H and O−H regions recorded before and after the introduction of $\beta$-Gal indicated that bound water molecules were not replaced by enzyme,[82] showing that adsorption of enzyme on the Mal-EG4 SAM by physical interactions was unlikely.

*3.2.2. Evidence of Direct Single-Point Chemical Attachment of Cysteine-Modified $\beta$-Gal to the Mal-EG4 SAM.* Figure 3 shows SFG ssp spectra from the maleimide-terminated SAM−buffer solution interface recorded in the absence of $\beta$-Gal-V152C (black spectrum). A weak SFG signal was detected from the maleimide groups of the SAM with a peak centered around 1620 cm$^{-1}$. After the maleimide-terminated surface was incubated with $\beta$-Gal-V152C, an SFG amide-I signal centered at ∼1650 cm$^{-1}$ was observed (Figure 3, red spectrum). SFG spectra were again collected after the interface was extensively washed with buffer to remove any non-covalently adsorbed protein. The SFG signal did not noticeably change after washing, consistent with the conclusion that $\beta$-Gal-V152C molecules were chemically immobilized on the Mal-EG4 surface (Figure 3, blue spectrum). The spectrum is dominated by the peak at ∼1650 cm$^{-1}$, which is contributed by the $\alpha$-helical components, and a peak at ∼1635 cm$^{-1}$, which is contributed by the $\beta$-sheet components in $\beta$-Gal immobilized at the SAM−protein solution interface.

*3.2.3. Orientation Determination. 3.2.3.1. SFG Results.* In addition to the ssp SFG spectrum, the SFG ppp spectrum was

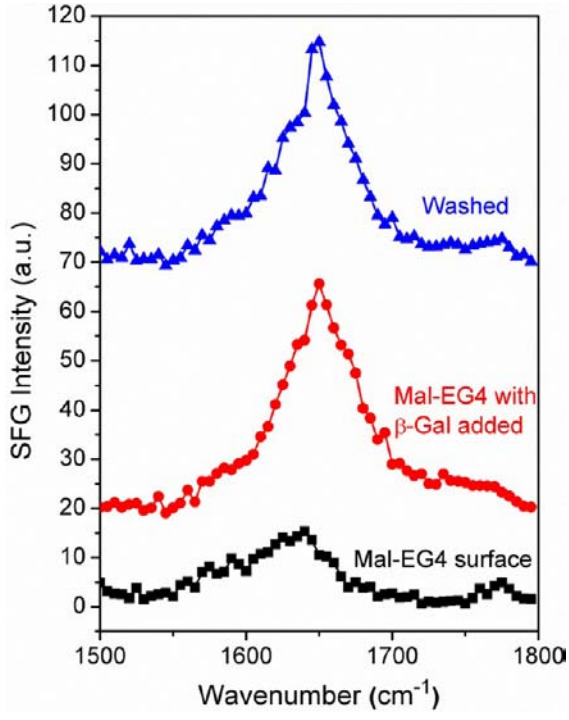


**Figure 3.** SFG ssp spectra collected from the Mal-EG4 SAM−buffer solution interface before (black ■) and after (red ●) the addition of $\beta$-Gal-V152C. A strong SFG signal was observed after the addition of $\beta$-Gal-V152C, indicating surface immobilization. The SFG signal remained the same after the interface was washed with buffer (blue ▲), showing that chemical immobilization occurred.

also collected for $\beta$-Gal-V152C chemically immobilized on the maleimide-terminated SAM. Both spectra are shown in Figure 4A. After the spectra were fit, the $\chi_{ppp}/\chi_{ssp}$ ratio at 1650 cm$^{-1}$ was determined to be 1.70. The fitting parameters are shown in Table 1. After corrections for the effects of Fresnel coefficients on the two polarization combinations were made, it was deduced that the measured $\chi_{zzz}/\chi_{xxz}$ value was 1.91 for the immobilized $\beta$-Gal. As shown in ref 56, plotting this value on the theoretical contour map of $\chi_{zzz}/\chi_{xxz}$ (calculated as a function of the tilt and twist angles for this enzyme using the computer software[56] based on the $\beta$-Gal crystal structure)


dx.doi.org/10.1021/ja403672s | J. Am. Chem. Soc. 2013, 135, 12660−12669

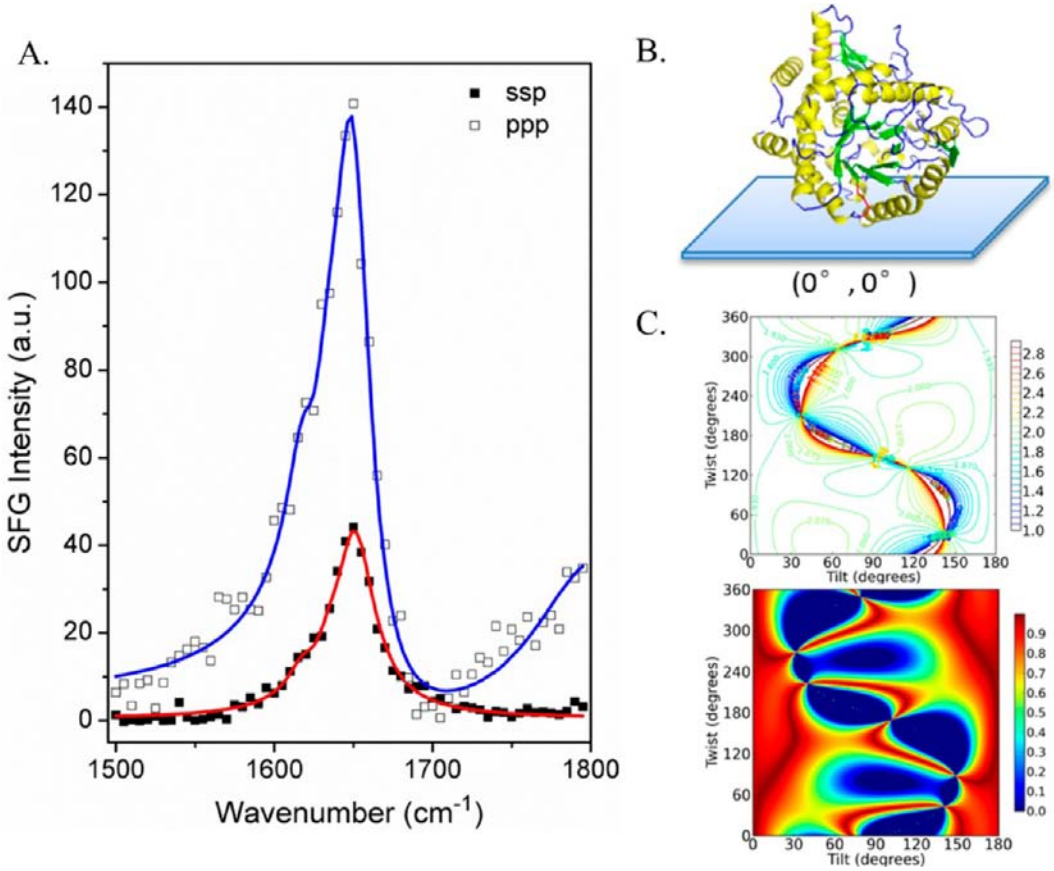


**Figure 4.** (A) SFG ssp (■, red line) and ppp (□, blue line) spectra collected from $\beta$-Gal-V152C immobilized at the Mal-EG4 SAM−solution interface. Squares are experimental data; lines are fit results. (B) Orientation of $\beta$-Gal with (tilt angle, twist angle) = (0°, 0°). The cysteine-functionalized site is shown in red, and the SAM is shown as a blue plane. (C) Top: Dependence of the SFG $\chi_{zzz}/\chi_{xxz}$ ratio on the tilt and twist angles of $\beta$-Gal-V152C calculated using the newly developed computer package.[56] Bottom: Possible orientation angle regions deduced on the basis of the experimentally measured $\chi_{zzz}/\chi_{xxz}$ ratio of $\beta$-Gal-V152C. Colors indicate the quality of the match (1 = exact).

**Table 1. SFG Fitting Parameters**

| SAM | polarization combinations | peak center ($cm^{-1}$) | peak width ($cm^{-1}$) | signal strength | assignment |
|---|---|---|---|---|---|
| Mal-EG4 | ssp | 1620 | 10.0 | 10.7 | maleimide C═O groups from SAM |
| | | 1635 | 10.0 | 10.7 | $\beta$-sheets in $\beta$-Gal |
| | | 1650 | 15.0 | 91.0 | $\alpha$-helices in $\beta$-Gal |
| | ppp | 1620 | 10.0 | 18.0 | maleimide C═O groups from SAM |
| | | 1635 | 10.0 | 15.4 | $\beta$-sheets in $\beta$-Gal |
| | | 1650 | 15.0 | 154 | $\alpha$-helices in $\beta$-Gal |
| OTS | ssp | 1600 | 15.0 | 11.3 | side chains in $\beta$-Gal |
| | | 1625 | 10.0 | 6.81 | $\beta$-sheets in $\beta$-Gal |
| | | 1644 | 15.0 | 37.5 | random $\beta$-Gal structure |
| | | 1650 | 16.0 | 55.3 | $\alpha$-helices in $\beta$-Gal |
| | | 1680 | 10.0 | 14.2 | $\beta$-sheets in $\beta$-Gal |
| | | 1710 | 10.0 | 15.4 | side chains in $\beta$-Gal |
| | ppp | 1600 | 15.0 | 12.1 | side chains in $\beta$-Gal |
| | | 1625 | 10.0 | 19.9 | $\beta$-sheets in $\beta$-Gal |
| | | 1644 | 15.0 | 43.4 | random $\beta$-Gal structure |
| | | 1650 | 16.0 | 106 | $\alpha$-helices in $\beta$-Gal |
| | | 1680 | 10.0 | 15.9 | $\beta$-sheets in $\beta$-Gal |
| | | 1710 | 10.0 | 27.9 | side chains in $\beta$-Gal |

allowed us to deduce the possible orientation regions of the immobilized $\beta$-Gal at the Mal-EG4 SAM−enzyme solution interface (Figure 4C). In the orientation determination, the enzyme reference position [(tilt angle, twist angle) = (0°, 0°)] was defined using a $\beta$-Gal orientation in which the surface cysteine residue was chemically bound to the surface maleimide group (Figure 4B).

Figure 4C indicates that many tilt and twist angle combinations can satisfy the deduced experimental results. To place more constraints and thus narrow down the possible orientations for $\beta$-Gal at the interface, we incorporated the polarized ATR-FTIR measurements as discussed below. SFG and ATR-FTIR measure different structural information, so these measurements provided independent information on the protein orientation.[55,66]

*3.2.3.2. ATR-FTIR Results.* ATR-FTIR spectra were collected using p-polarized and s-polarized IR beams (Figure 5A). Polarized ATR-FTIR spectra have been used to study peptide and protein orientations.[51,52] Especially, the amide-I ATR-FTIR spectra (mainly contributed by the backbone C═O stretches) were chosen for analysis because the amide-I signals have different peak centers for different protein secondary structures, as has been discussed in detail in the literature.[51,52] When the amide-I ATR-FTIR spectra are fit using Gaussian peaks, the peak centers can be directly correlated with the secondary structures contained in a protein. The ATR-FTIR spectra in Figure 5A were fit (Table 2), and the dichroic ratio for the


dx.doi.org/10.1021/ja403672s | J. Am. Chem. Soc. 2013, 135, 12660−12669

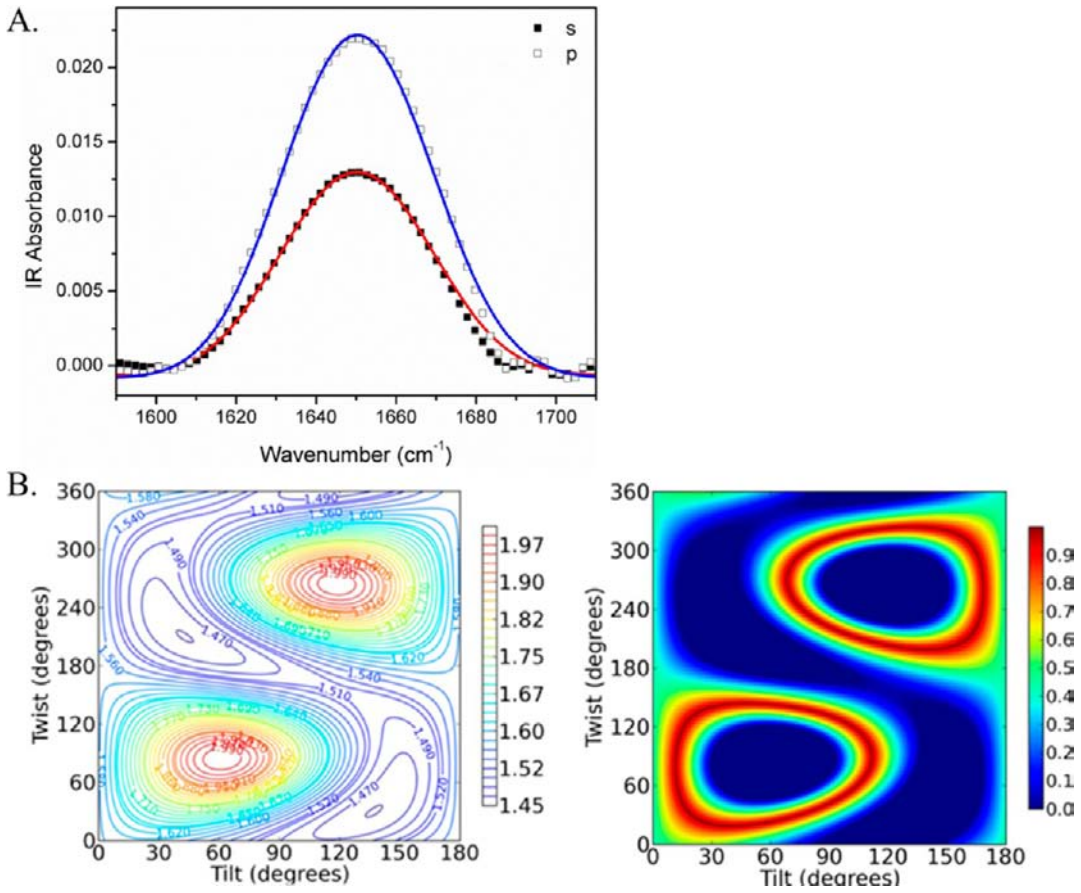


**Figure 5.** (A) ATR-FTIR spectra collected from $\beta$-Gal-V152C immobilized at the Mal-EG4 SAM−solution interface using p (□, blue line) and s (■, red line) polarizations. Squares are experimental data; lines are fitting results. (B) Left: Dependence of the ATR-FTIR dichroic ratio $R^{ATR}$ on the tilt and twist angles of $\beta$-Gal-V152C calculated using the newly developed computer package.[56] Right: Possible orientation angle regions deduced on the basis of the experimentally measured $R^{ATR}$ value for $\beta$-Gal-V152C. Colors indicate the quality of the match (1 = exact).

**Table 2. ATR-FTIR Fitting Parameters**

| polarization | peak center ($cm^{-1}$) | peak width ($cm^{-1}$) | intensity | assignment |
|---|---|---|---|---|
| s | 1631 | 10.0 | 0.00171 | $\beta$-sheets in $\beta$-Gal |
| | 1640 | 10.0 | 0.00286 | random coils in $\beta$-Gal |
| | 1655 | 12.0 | 0.0112 | $\alpha$-helices in $\beta$-Gal |
| p | 1631 | 10.0 | 0.00211 | $\beta$-sheets in $\beta$-Gal |
| | 1640 | 10.0 | 0.00542 | random coils in $\beta$-Gal |
| | 1655 | 12.0 | 0.0187 | $\alpha$-helices in $\beta$-Gal |

signal at ~1655 $cm^{-1}$, which is attributed to $\alpha$-helical components of $\beta$-Gal, was calculated to be $R^{ATR}$ = 1.67. Unlike SFG, ATR-FTIR is not inherently sensitive to ordered structures (e.g., $\alpha$-helices), and consequently, the ATR-FTIR spectra contained more vibrational peak centers corresponding to additional secondary structures (e.g., a random-coil peak at 1644 $cm^{-1}$). The fitting results showed that the ATR-FTIR spectra contained contributions from $\alpha$-helix, $\beta$-sheet, and random coil structures in this immobilized enzyme. Similar to the SFG data analysis, the theoretical ATR-FTIR signal response from $\beta$-Gal was also calculated as a function of the tilt and twist angles.[56] From the computed ATR-FTIR response and the experimentally deduced $R^{ATR}$ of 1.67, the possible combinations of the tilt and twist angles of the immobilized $\beta$-Gal at the Mal-EG4 SAM−enzyme solution interface were deduced (Figure 5B). Similar to the SFG results, many possible combinations of the tilt and twist angles can satisfy the experimental data, so a unique orientation of $\beta$-Gal with respect to the interface could not be determined by ATR-FTIR alone.

*3.2.3.3. Combining Orientational Constraints from SFG and ATR-FTIR.* Overlapping the possible orientation angle regions deduced from the SFG and ATR-FTIR measurements (Figure 6) showed that there are only six regions in which the possible orientation angle combinations could satisfy both SFG and ATR-FTIR measurements. Furthermore, because the cysteine residue in $\beta$-Gal was in contact with the SAM surface, we could exclude the possible orientations with tilt angles larger than 90°. If we choose the best matches between the experimentally measured data and the calculated orientations for the regions with tilt angles smaller than 90°, we have one large area (an arc) with possible tilt angles ranging from 15° to 30° and twist angles ranging from 60° to 130° along with a very small region with a tilt angle of around 75° and a twist angle of around 30° (Figure 6, right plot). In Figure 7 we have plotted two representative orientations from the first arc region and one orientation from the latter small angle region along with three other representative orientations with tilt angles larger than 90°. We believe that the orientations shown in Figure 7a,b are the most likely orientations because they are consistent with the intended orientation that would arise by chemical immobilization of the enzyme on the SAM through binding of the enzyme cysteine side chain to the surface maleimide


dx.doi.org/10.1021/ja403672s | J. Am. Chem. Soc. 2013, 135, 12660−12669

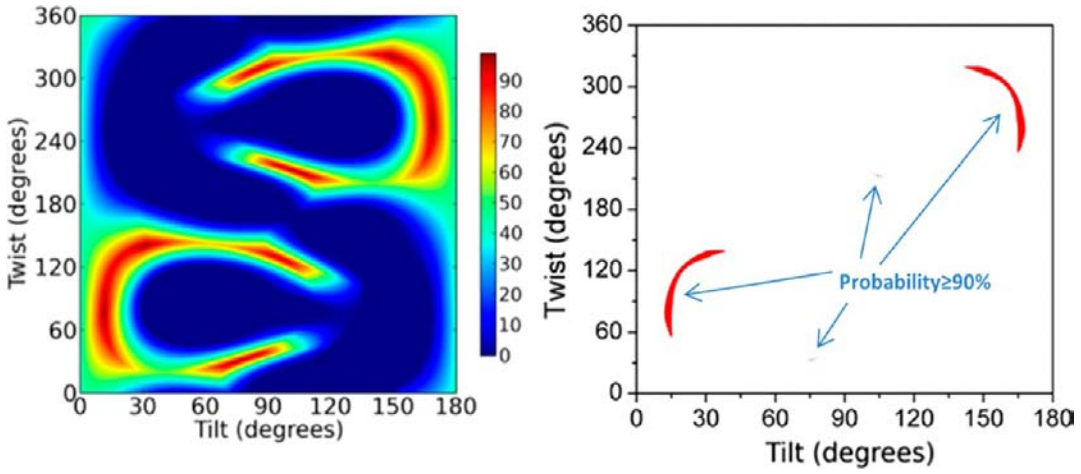


**Figure 6.** (left) Possible orientation angle regions deduced on the basis of both the SFG and ATR-FTIR measurements. Colors indicate the quality of the match (100% = exact). (right) Plot showing the possible orientation angles with probability ≥90% in red.

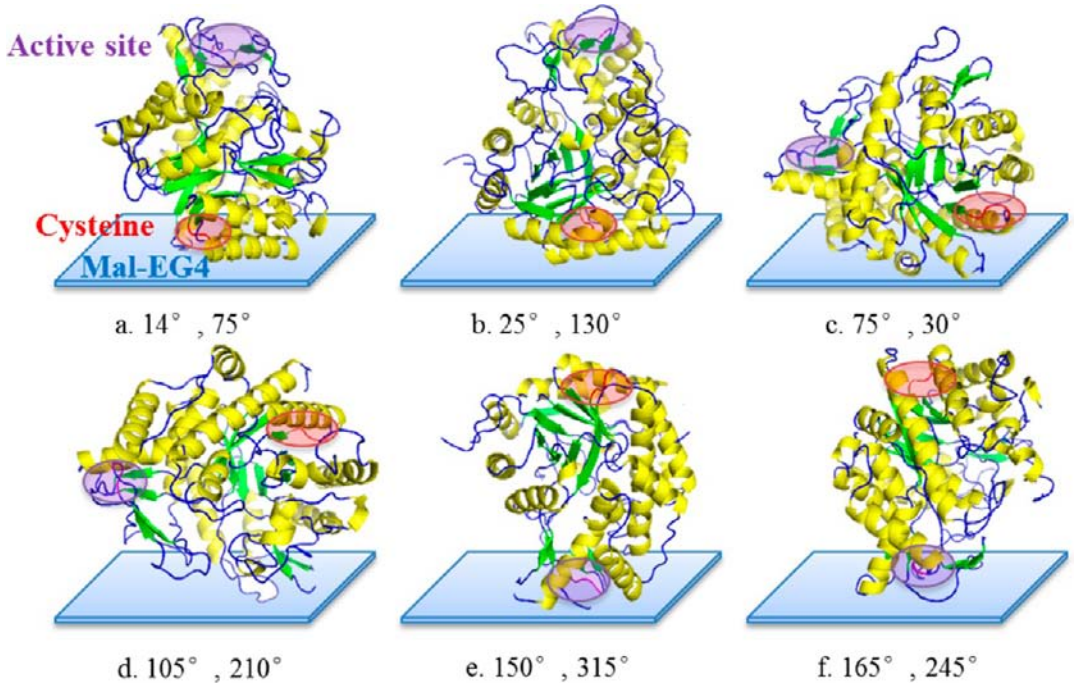


**Figure 7.** Possible orientations of immobilized β-Gal, with angles shown in the format of (tilt angle, twist angle). The most likely orientations are (a) (14°, 75°) and (b) (25°, 130°) because they are well-correlated to the designed orientation in which the chemical immobilization is achieved through binding of the enzyme cysteine group and a surface maleimide group.

groups. As shown in Figure 6, the possible angle region corresponding to the orientations shown in Figure 7a,b is much larger than the one corresponding to the orientation shown in Figure 7c, which also implies that the probability that the protein adopts orientations similar to those shown in Figure 7a,b is much higher than that for the structure shown in Figure 7c.

**3.3. SFG Studies of β-Gal on an OTS SAM.** SFG ssp spectra in the amide-I region were collected from the interface between an OTS SAM and the buffer solution before and after the addition of β-Gal into the buffer solution (Figure 8a). Before the introduction of β-Gal, no signal was detected. The increase in the SFG signal in the amide-I spectral region after the introduction of β-Gal into the buffer solution was attributed to β-Gal adsorbed at the OTS SAM–buffer solution interface. Additional peaks due to from side chains (1600 and 1710 $cm^{-1}$), random structures (1644 $cm^{-1}$), and β-sheets (1680 $cm^{-1}$) also showed up. The appearance of these side chains and secondary structures of β-Gal on the OTS SAM is most likely caused by partial unfolding of the enzyme to expose hydrophobic residues that physically adsorb on the hydrophobic OTS SAM surface through hydrophobic interactions.[48,83] A similar SFG spectrum was detected at the OTS–solution interface for the "no cysteine" β-Gal enzyme (data not shown), indicating that the cysteine does not greatly alter the physical adsorption on the OTS SAM surface. An SFG spectrum was also collected after the surface was washed with pure buffer solution (Figure 8a). The spectral intensity decreased, showing that some loosely adsorbed proteins were washed off the OTS SAM surface. As discussed below, the


dx.doi.org/10.1021/ja403672s | J. Am. Chem. Soc. 2013, 135, 12660–12669

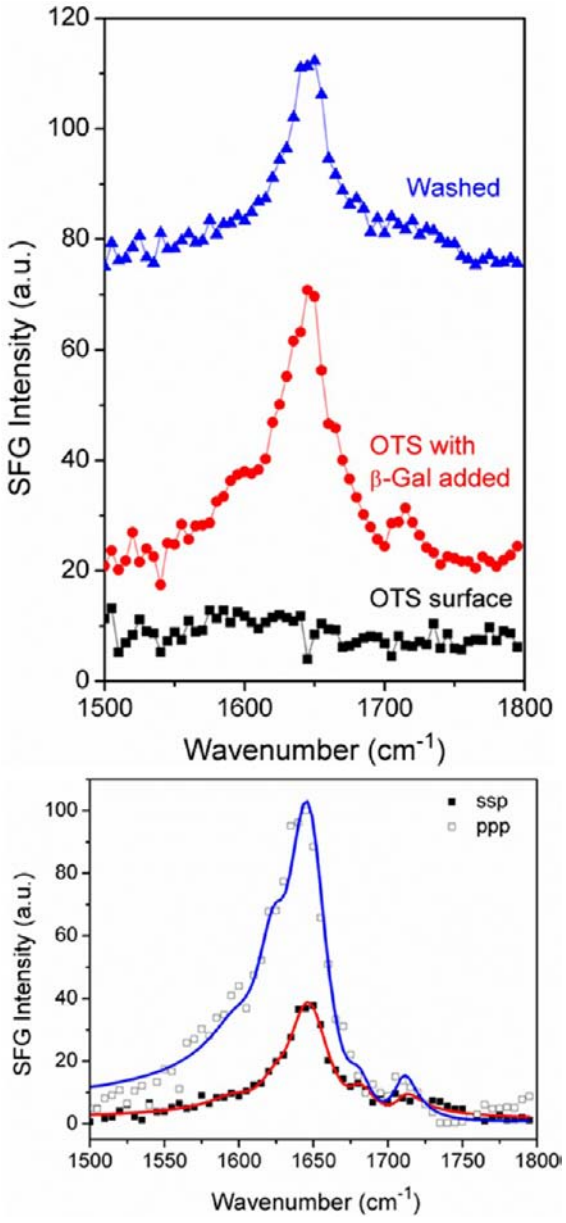


**Figure 8.** Top: SFG ssp spectra collected from the OTS SAM–buffer solution interface before (black) and after (red) the addition of $\beta$-Gal-V152C to the buffer. After washing, SFG signal (blue) decreased, showing that some loosely adsorbed enzyme molecules were washed off. Bottom: SFG ssp (■, red line) and ppp (□, blue line) spectra collected from the OTS SAM–buffer solution interface after the addition of $\beta$-Gal-V152C. Squares are experimental data; lines are fitting results.

physically adsorbed $\beta$-Gal had much reduced activity relative to the chemically immobilized enzyme.

**3.4. Activity of Surface-Immobilized $\beta$-Gal.** Although $\beta$-Gal has favorable structural features for determining its surface orientation by SFG, the enzyme was not sufficiently active that we could directly measure the $\beta$-Gal activity on the prism surfaces used for SFG measurements. To enhance the sensitivity, we attached the enzyme to glass beads coated with either a Mal-EG4 or OTS SAM. On a microscopic level, the SAMs on the bead surfaces should be chemically identical to that on the SFG prism, but the total surface area should be greatly increased. To increase the sensitivity further, the fluorogenic substrate FDG was used to measure the activity (see Materials and Methods).

With this substrate, the specific activity of free $\beta$-Gal-V152C in solution was 1.1 nmol $min^{-1}$ $mg^{-1}$ (Figure 9). The specific

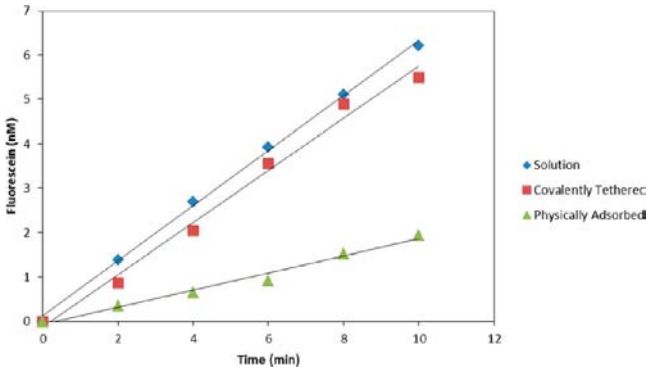


**Figure 9.** Activities of $\beta$-Gal-V152C free in solution (blue), covalently tethered to the EG4-Mal SAM via the single engineered cysteine at position 152 (red), and physically adsorbed to the hydrophobic OTS SAM (green). In each case, 10 pmol of $\beta$-Gal-V152C was added to 1 mL of solution.

activity of $\beta$-Gal-V152C immobilized on Mal-EG4-derivatized glass beads was 1.08 nmol $min^{-1}$ $mg^{-1}$, which was identical to that of the free enzyme in solution within the experimental error. In contrast, the specific activity of $\beta$-Gal-V152C physically adsorbed on OTS-derivatized beads was 0.35 nmol $min^{-1}$ $mg^{-1}$, which is only one-third that of the free enzyme in solution.

To determine the specific activities of immobilized and free enzyme, the amount of enzyme attached to the glass beads was quantified by reaction with bicinchoninic acid (see the Supporting Information). This allowed us to compare the loading of the beads with that expected for an ideal monolayer. On the basis of a bead diameter of 75 $\mu$m and a footprint of ~100 $nm^2$ for $\beta$-Gal, monolayer coverage would result in a loading of ~0.27 pmol of enzyme/mg of beads. The experimentally determined protein loading for $\beta$-Gal-V152C immobilized through the Mal-EG4 linker was 0.14 pmol/mg of beads, suggesting that the specifically tethered enzymes likely were attached as a monolayer with few or no non-covalent interactions between enzyme molecules. For enzyme physically adsorbed on OTS-derivatized beads, the loading was 1.0 pmol/mg of beads, which is much larger than the concentration expected for a monolayer. This suggests that protein–protein interactions between physically adsorbed enzyme molecules were likely to occur, and this may be part of the reason that the activity of the physically adsorbed enzyme was much lower.

It is interesting that we observed a stronger SFG signal intensity for $\beta$-Gal-V152C immobilized through the Mal-EG4 linker than for $\beta$-Gal-V152C physically adsorbed on OTS even though the surface coverage of the latter was higher. The SFG signal intensity is related to the surface coverage and the orientation of functional groups or molecules (under the fixed visible and IR input beam energies). With chemical immobilization, the enzyme molecules more or less adopted a similar orientation with the cysteine group facing the surface for immobilization, enabling the signal to be stronger. The signal should be proportional to the square of the surface coverage (assuming that the orientation is coverage-independent, which is likely for chemical immobilization). For the physically


dx.doi.org/10.1021/ja403672s | J. Am. Chem. Soc. 2013, 135, 12660–12669

adsorbed enzyme molecules, the orientation distribution can be much broader. Therefore, SFG signals from enzyme molecules with different orientations can cancel to some extent. As a result, the detected SFG signal can be smaller even when the enzyme surface coverage is higher.

## 4. CONCLUSION

In this work, specific immobilization of 6-phospho-$\beta$-galactosidase on SAMs containing maleimide end groups and oligo(ethylene glycol) spacer segments was achieved through a unique cysteinyl residue. The possible orientations of the immobilized $\beta$-Gal were determined to be in a region with tilt angles ranging from 15° to 30° and twist angles ranging from 60° to 130° by combining two independent vibrational spectroscopic techniques. The activity of the immobilized enzyme was not reduced by surface attachment, in agreement with the outward-facing orientation of the active site as deduced from combined SFG and ATR-FTIR measurements. On the other hand, 6-phospho-$\beta$-galactosidase nonspecifically adsorbed onto hydrophobic octadecyl SAMs appeared to be partially denatured and exhibited significantly reduced activity. As discussed above, in our SFG and ATR-FTIR studies, we assumed that the specifically immobilized enzymes did not significantly change their structures. Since the activity of the chemically immobilized $\beta$-Gal was similar to that in solution and the enzyme orientation determined spectroscopically is reasonable, we believe that this assumption, at least in this case, is valid. In future experiments, we aim to further characterize the possible conformational changes of surface-tethered proteins using isotope-labeled proteins.

A detailed correlation between the directly measured orientation and activity of a surface-attached enzyme has seldom been previously reported. This work provides a systematic means to characterize the interfacial orientation of immobilized enzymes, leading to fundamental knowledge regarding which properties of an enzyme may be altered by tethering without compromising its function. In the future, this will impact the development of an increasingly wide range of devices that use surface-immobilized enzymes as integral components with improved functions, better sensitivity, enhanced stability, and longer shelf life.

## ■ ASSOCIATED CONTENT

### Supporting Information

Detailed experiments on thiol determination of $\beta$-Gal, immobilization on glass beads, surface concentration determination, SAM characterization, and ATR-FTIR experiments performed on the OTS surface. This material is available free of charge via the Internet at http://pubs.acs.org.

## ■ AUTHOR INFORMATION

### Corresponding Author

nmarsh@umich.edu; zhanc@umich.edu

### Notes

The authors declare no competing financial interest.

## ■ ACKNOWLEDGMENTS

This work was supported by the Defense Threat Reduction Agency (HDTRA1-11-1-0019) and the Army Research Office (W911NF-11-1-0251). We thank Dr. Fugen Wu for depositing $SiO_2$ on $CaF_2$, Dr. Lei Shen for help with enzyme orientation analysis and collection of SFG spectra of the OTS SAM, Dr. Kai Sun from EMAL for useful discussions concerning the XPS experiments and data analysis, the Lurie Nanofabrication Facility at the University of Michigan for $SiO_2$ deposition, and Dr. Bharat Kumar and Scott Crittenden for characterizing the Mal-EG4 SAM using AFM.

## ■ REFERENCES

(1) Brady, D.; Jordaan, J. *Biotechnol. Lett.* **2009**, *31*, 1639.
(2) Cao, L. Q. *Curr. Opin. Chem. Biol.* **2005**, *9*, 217.
(3) Hanefeld, U.; Gardossi, L.; Magner, E. *Chem. Soc. Rev.* **2009**, *38*, 453.
(4) Tischer, W.; Wedekind, F. *Top. Curr. Chem.* **1999**, *200*, 95.
(5) Ansari, S. A.; Husain, Q. *Biotechnol. Adv.* **2012**, *30*, 512.
(6) Cordeiro, A. L.; Hippius, C.; Werner, C. *Biotechnol. Lett.* **2011**, *33*, 1897.
(7) Frasconi, M.; Mazzei, F.; Ferri, T. *Anal. Bioanal. Chem.* **2010**, *398*, 1545.
(8) Jonkheijm, P.; Weinrich, D.; Schroder, H.; Niemeyer, C. M.; Waldmann, H. *Angew. Chem., Int. Ed.* **2008**, *47*, 9618.
(9) Kristensen, J. B.; Meyer, R. L.; Laursen, B. S.; Shipovskov, S.; Besenbacher, F.; Poulsen, C. H. *Biotechnol. Adv.* **2008**, *26*, 471.
(10) Lee, S. Y.; Lee, J.; Chang, J. H.; Lee, J. H. *BMB Rep.* **2011**, *44*, 77.
(11) Noah, N. M.; Omole, M.; Stern, S.; Zhang, S. Y.; Sadik, O. A.; Hess, E. H.; Martinovic, J.; Baker, P. G. L.; Iwuoha, E. I. *Anal. Biochem.* **2012**, *428*, 54.
(12) Olsen, S. M.; Pedersen, L. T.; Laursen, M. H.; Kiil, S.; Dam-Johansen, K. *Biofouling* **2007**, *23*, 369.
(13) Rodrigues, R. C.; Berenguer-Murcia, A.; Fernandez-Lafuente, R. *Adv. Synth. Catal.* **2011**, *353*, 2216.
(14) Tasso, M.; Pettitt, M. E.; Cordeiro, A. L.; Callow, M. E.; Callow, J. A.; Werner, C. *Biofouling* **2009**, *25*, 505.
(15) Veluchamy, P.; Sivakumar, P. M.; Doble, M. *J. Agric. Food. Chem.* **2011**, *59*, 10869.
(16) Halamkova, L.; Halamek, J.; Bocharova, V.; Szczupak, A.; Alfonta, L.; Katz, E. *J. Am. Chem. Soc.* **2012**, *134*, 5040.
(17) Sassolas, A.; Blum, L. J.; Leca-Bouvier, B. D. *Biotechnol. Adv.* **2012**, *30*, 489.
(18) Tasso, M.; Conlan, S. L.; Clare, A. S.; Werner, C. *Adv. Funct. Mater.* **2012**, *22*, 39.
(19) Wang, Z. G.; Wan, L. S.; Liu, Z. M.; Huang, X. J.; Xu, Z. K. *J. Mol. Catal. B: Enzym.* **2009**, *56*, 189.
(20) Klein, M. P.; Nunes, M. R.; Rodrigues, R. C.; Benvenutti, E. V.; Costa, T. M. H.; Hertz, P. F.; Ninow, J. L. *Biomacromolecules* **2012**, *13*, 2456.
(21) Garcia-Galan, C.; Berenguer-Murcia, A.; Fernandez-Lafuente, R.; Rodrigues, R. C. *Adv. Synth. Catal.* **2011**, *353*, 2885.
(22) Butler, J. E. *Methods* **2000**, *22*, 4.
(23) You, C. C.; De, M.; Han, G.; Rotello, V. M. *J. Am. Chem. Soc.* **2005**, *127*, 12873.
(24) Talbert, J. N.; Goddard, J. M. *Colloids Surf., B* **2012**, *93*, 8.
(25) Shen, Y. R. *Nature* **1989**, *337*, 519.
(26) Eisenthal, K. B. *Chem. Rev.* **1996**, *96*, 1343.
(27) Richmond, G. L. *Chem. Rev.* **2002**, *102*, 2693.
(28) Liu, J.; Conboy, J. C. *J. Am. Chem. Soc.* **2004**, *126*, 8376.
(29) Ye, H. K.; Abu-Akeel, A.; Huang, J.; Katz, H. E.; Gracias, D. H. *J. Am. Chem. Soc.* **2006**, *128*, 6528.
(30) Chen, X.; Yang, T.; Kataoka, S.; Cremer, P. S. *J. Am. Chem. Soc.* **2007**, *129*, 12272.
(31) Li, Q. F.; Kuo, C. W.; Yang, Z.; Chen, P. L.; Chou, K. C. *Phys. Chem. Chem. Phys.* **2009**, *11*, 3436.
(32) Yang, Z.; Li, Q. F.; Gray, M. R.; Chou, K. C. *Langmuir* **2010**, *26*, 16397.
(33) Humbert, C.; Busson, B. In *Biointerface Characterization by Advanced IR Spectroscopy*; Pradier, C. M., Chabal, Y. J., Eds.; Elsevier: Amsterdam, 2011; p 279.
(34) Chen, X.; Wang, J.; Sniadecki, J. J.; Even, M. A.; Chen, Z. *Langmuir* **2005**, *21*, 2662.

(35) Wang, J.; Chen, X.; Clarke, M. L.; Chen, Z. *Proc. Natl. Acad. Sci. U.S.A.* **2005**, *102*, 4978.
(36) Chen, X.; Chen, Z. *Biochim. Biophys. Acta* **2006**, *1758*, 1257.
(37) Chen, X.; Tang, H. Z.; Even, M. A.; Wang, J.; Tew, G. N.; Chen, Z. *J. Am. Chem. Soc.* **2006**, *128*, 2711.
(38) Chen, X.; Boughton, A. P.; Tesmer, J. J. G.; Chen, Z. *J. Am. Chem. Soc.* **2007**, *129*, 12658.
(39) Ye, S. J.; Nguyen, K. T.; Le Clair, S. V.; Chen, Z. *J. Struct. Biol.* **2009**, *168*, 61.
(40) Nguyen, K. T.; King, J. T.; Chen, Z. *J. Phys. Chem. B* **2010**, *114*, 8291.
(41) Boughton, A. P.; Yang, P.; Tesmer, V. M.; Ding, B.; Tesmer, J. J. G.; Chen, Z. *Proc. Natl. Acad. Sci. U.S.A.* **2011**, *108*, E667.
(42) Liu, Y.; Jasensky, J.; Chen, Z. *Langmuir* **2012**, *28*, 2113.
(43) Baugh, L.; Weidner, T.; Baio, J. E.; Nguyen, P.-C. T.; Gamble, L. J.; Stayton, P. S.; Castner, D. G. *Langmuir* **2010**, *26*, 16434.
(44) Fu, L.; Ma, G.; Yan, E. C. Y. *J. Am. Chem. Soc.* **2010**, *132*, 5405.
(45) Fu, L.; Liu, J.; Yan, E. C. Y. *J. Am. Chem. Soc.* **2011**, *133*, 8094.
(46) Chen, X.; Sagle, L. B.; Cremer, P. S. *J. Am. Chem. Soc.* **2007**, *129*, 15104.
(47) Kim, J.; Cremer, P. S. *ChemPhysChem* **2001**, *2*, 543.
(48) Kim, J.; Somorjai, G. A. *J. Am. Chem. Soc.* **2003**, *125*, 3150.
(49) Weidner, T.; Breen, N. F.; Li, K.; Drobny, G. P.; Castner, D. G. *Proc. Natl. Acad. Sci. U.S.A.* **2010**, *107*, 13288.
(50) Baio, J. E.; Weidner, T.; Baugh, L.; Gamble, L. J.; Stayton, P. S.; Castner, D. G. *Langmuir* **2012**, *28*, 2107.
(51) Tatulian, S. A.; Jones, L. R.; Reddy, L. G.; Stokes, D. L.; Tamm, L. K. *Biochemistry* **1995**, *34*, 4448.
(52) Cerf, E.; Sarroukh, R.; Tamamizu-Kato, S.; Breydo, L.; Derclaye, S.; Dufrêne, Y. F.; Narayanaswami, V.; Goormaghtigh, E.; Ruysschaert, J. M.; Raussens, V. *Biochem. J.* **2009**, *421*, 415.
(53) Ye, S. J.; Li, H.; Wei, F.; Jasensky, J.; Boughton, A. P.; Yang, P.; Chen, Z. *J. Am. Chem. Soc.* **2012**, *134*, 6237.
(54) Barlow, D. E.; Wahl, K. J. *Annu. Rev. Anal. Chem.* **2012**, *5*, 229.
(55) Wang, J.; Paszti, Z.; Clarke, M. L.; Chen, X.; Chen, Z. *J. Phys. Chem. B* **2007**, *111*, 6088.
(56) Yang, P.; Boughton, A.; Homan, K.; Tesmer, J.; Chen, Z. *J. Am. Chem. Soc.* **2013**, *135*, 5044.
(57) Ding, B.; Chen, Z. *J. Phys. Chem. B* **2012**, *116*, 2545.
(58) Wiesmann, C.; Hengstenberg, W.; Schulz, G. E. *J. Mol. Biol.* **1997**, *269*, 851.
(59) Chaki, N. K.; Vijayamohanan, K. *Biosens. Bioelectron.* **2002**, *17*, 1.
(60) Houseman, B. T.; Gawalt, E. S.; Mrksich, M. *Langmuir* **2003**, *19*, 1522.
(61) Uzarski, J. R.; Mello, C. M. *Anal. Chem.* **2012**, *84*, 7359.
(62) Wang, J.; Buck, S. M.; Even, M. A.; Chen, Z. *J. Am. Chem. Soc.* **2002**, *124*, 13302.
(63) Wang, J.; Even, M. A.; Chen, X.; Schmaier, A. H.; Waite, J. H.; Chen, Z. *J. Am. Chem. Soc.* **2003**, *125*, 9914.
(64) Wang, J.; Paszti, Z.; Even, M. A.; Chen, Z. *J. Phys. Chem. B* **2004**, *108*, 3625.
(65) Chen, X.; Clarke, M. L.; Wang, J.; Chen, Z. *Int. J. Mod. Phys. B* **2005**, *19*, 691.
(66) Chen, X.; Wang, J.; Boughton, A. P.; Kristalyn, C. B.; Chen, Z. *J. Am. Chem. Soc.* **2007**, *129*, 1420.
(67) Chen, X.; Wang, J.; Kristalyn, C. B.; Chen, Z. *Biophys. J.* **2007**, *93*, 866.
(68) Nguyen, K. T.; Le Clair, S. V.; Ye, S. J.; Chen, Z. *J. Phys. Chem. B* **2009**, *113*, 12358.
(69) Nguyen, K. T.; Le Clair, S. V.; Ye, S. J.; Chen, Z. *J. Phys. Chem. B* **2009**, *113*, 12169.
(70) Yang, P.; Ramamoorthy, A.; Chen, Z. *Langmuir* **2011**, *27*, 7760.
(71) Bayramoglu, G.; Tunali, Y.; Arica, M. Y. *Catal. Commun.* **2007**, *8*, 1094.
(72) Eldin, M. S. M.; Elaassar, M. R.; Elzatahry, A. A.; Al-Sabah, M. M. B.; Hassan, E. A. *J. Appl. Polym. Sci.* **2012**, *125*, 1724.
(73) Elnashar, M. M. M.; Yassin, M. A. *J. Appl. Polym. Sci.* **2009**, *114*, 17.
(74) López-Gallego, F.; Betancor, L.; Hidalgo, A.; Alonso, N.; Fernandez-Lorente, G.; Guisan, J. M.; Fernandez-Lafuente, R. *Enzyme Microb. Technol.* **2005**, *37*, 750.
(75) López-Gallego, F.; Betancor, L.; Mateo, C.; Hidalgo, A.; Alonso-Morales, N.; Dellamora-Ortiz, G.; Guisán, J. M.; Fernández-Lafuente, R. *J. Biotechnol.* **2005**, *119*, 70.
(76) Grosova, Z.; Rosenberg, M.; Rebros, M.; Sipocz, M.; Sedlackova, B. *Biotechnol. Lett.* **2008**, *30*, 763.
(77) Taqieddin, E.; Amiji, M. *Biomaterials* **2004**, *25*, 1937.
(78) Herrwerth, S.; Eck, W.; Reinhardt, S.; Grunze, M. *J. Am. Chem. Soc.* **2003**, *125*, 9359.
(79) Hoffmann, C.; Tovar, G. E. M. *J. Colloid Interface Sci.* **2006**, *295*, 427.
(80) Zheng, J.; Li, L. Y.; Chen, S. F.; Jiang, S. Y. *Langmuir* **2004**, *20*, 8931.
(81) Li, L. Y.; Chen, S. F.; Zheng, J.; Ratner, B. D.; Jiang, S. Y. *J. Phys. Chem. B* **2005**, *109*, 2934.
(82) Stein, M. J.; Weidner, T.; McCrea, K.; Castner, D. G.; Ratner, B. D. *J. Phys. Chem. B* **2009**, *113*, 11550.
(83) Meadows, P. Y.; Walker, G. C. *Langmuir* **2005**, *21*, 4096.